DEVELOPMENT OF A COMPUTATIONAL MODEL APPLIED TO FORCED CONVECTION IN CYLINDRICAL AND D-SHAPED THERMAL TANKS

Darci Luiz Savicki, darcisavicki@furg.br
Ingrid Nunes Sabin, ingridsabin@bol.com.br
IMEF –Institute of Mathematics, Statistics and Physics - FURG – Federal University of Rio Grande
Av. Itália Km 8, CEP 96201-900, Rio Grande, RS, Brazil

Abstract. *Natural and forced convection in cylindrical and D-shaped tanks are numerically studied. In many applications cylindrical tanks, with aspect ratio L/D>>1, are used. In cases where the largest diameter allowed is limited in project and L/D>2.75, replacing the conventional cylindrical tank for a D-shaped one was found to have economical advantages, reducing the ratio surface area/volume. Numerical simulation was used to investigate the consequences of this replacement on the temperature and velocity fields in tanks applied to solar energy systems. The numerical results obtained in this work show that, in cases where the ratio aspect of the cylindrical tank is high, the D-shaped tanks have more advantageous characteristics than the usual cylindrical shape, which encourage its use.*
Keywords*: natural and forced convection, thermal tanks, water heating systems*

1. INTRODUCTION

One of the issues of interest in natural convection is the optimization of thermal energy storage equipment. An illustrative case is solar water heating systems, in which a good performance of the storage tank represents a considerable increase in the global efficiency. In such systems, one of the most desirable characteristics is an effective thermal stratification. The thermal stratification inside the tank depends on the velocity of the inlet jet as well as on the difference between the inlet and outlet temperatures of the collectors. There is a significant number of studies on the problem of natural convection inside vertical cylindrical cavities, but few works consider horizontal cylindrical cavities. Among the three-dimensional studies, Schneider and Straub (1992) investigated numerically the laminar natural convection in inclined cylindrical cavities, in which the top surface temperature was higher than the bottom surface temperature and the side wall was adiabatic.

Eames and Norton (1998) studied the influence of the inlet jet on thermal stratification of horizontal cylindrical tanks. They verified that, in the cases in which the hot water jet temperature was time-dependent, a better thermal stratification could be obtained by placing the inlets at different height positions. The use of devices to reduce the velocity of the inlet jet was also suggested. The use of devices such as baffle plates, diffuser tubes or perforated tubes can also be found in studies by other researchers. Alizadeh (1999) studied experimentally the charge and discharge processes as well as the influence of different types of diffusers (straight and conic) on the thermal stratification in horizontal tanks. The author found that it can be increased with the use of a divergent conical tube. Zachar *et al.* (2003) studied numerically the impact of a baffle plate facing the inlet jet on thermal stratification in vertical tanks. According to their study, the use of large baffle plates allows the preservation of the thermal stratification, even for high flow rates. Savicki *et al.* (2011) conducted a numerical-experimental investigation in horizontal cylindrical tanks, and obtained a satisfactory agreement between the numerical and the experimental results, proposing a correlation for the heat transfer coefficient and for degree of thermal stratification. Shah and Furbo (2003) performed a numerical study about the influence of inlet jets on the temperature stratification in vertical tanks, using a commercial CFD code. It was verified that for high flow rates above 10 l/min a better thermal stratification was obtained using a baffle plate in front of the inlet jet. Consul *et al.* (2004) used parallel computation and a multiblocks technique, with structured meshes, to simulate the charge and discharge process (hot water intake) and to investigate the flow influence on the thermal stratification. In this work natural and forced convection in cylindrical and D-shaped tanks are numerically studied, using numerical simulation.

2. PHYSICAL AND MATHEMATICAL MODEL

2.1. Some mathematical relationships between the tanks under study

In solar water heating systems, cylindrical tanks commonly have a much greater length than the diameter (Astrosol, 2011). The aspect ratio (r=L/D) of such tanks ranges from 2 to 5. In solar systems powered by thermosyphon, horizontal cylindrical tanks, with diameters exceeding 0.7 m, are used because the available space for accommodation below the roof is very limited, where a horizontal cylindrical tank is used for hot water storage, as shown in Figure 1. Therefore, in order to store a sufficient volume of water, these tanks may be longer than 3 m and have aspect ratio of about 5.

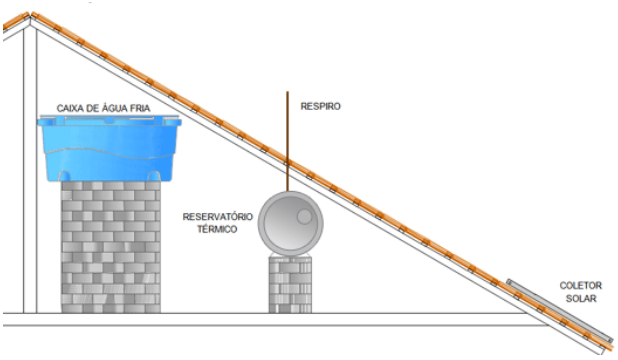

Figure 1. Thermosyphon Solar Water Heating System

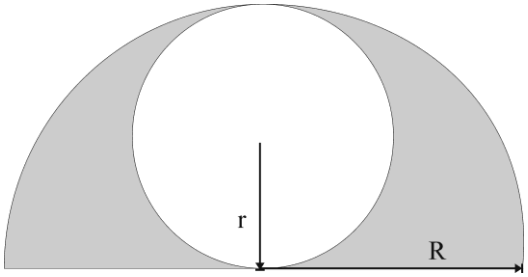

Figure 2. Cross section for cylindrical and D-shaped tanks

An alternative to avoiding too long tanks which has been little explored so far is the replacement of cylindrical geometry for another such as a D-shaped one, as shown in Figure 2. D-shaped tanks have some attractive characteristics, such as:

1- They allow storing the same volume as the conventional cylindrical tank, but using half-length (same height);
2- In cases where the conventional cylindrical tank shows high aspect ratio (above 2.75), they allow reducing heat losses, due to the reduction of the heat exchange area;
3- They are easy to be installed due to the flat bottom.

As a generic example, a cylindrical tank of r and z dimensions and a D-shaped tank of R=2r and Z dimensions are taken into account. For D-shaped tank to have the same external area as the cylindrical tank, its length should be

$$Z = \frac{\pi(z-r)}{\pi+2} \tag{1}$$

Moreover, in order to have the same volume as the cylindrical tank, D-shaped tank must have length of

$$Z = \frac{z}{2} \tag{2}$$

Equating (6) and (7) and evidencing the variable z, the following is obtained:

$$z = \frac{2\pi r}{\pi-2} \tag{3}$$

Finally, calculating the aspect ratio $ar = z/2r$, the maximum aspect ratio to make the tank cylindrical with a smaller surface area compared to D-shaped tank is found to be

$$ar = \frac{\pi}{\pi-2} \approx 2.752 \tag{4}$$

Thus, for example, for a cylindrical tank with radius 0.35 m and length 3.6 m ($ar \approx 5.1$), a corresponding D-shaped tank with R=0.7m and Z=1.8m would store the same volume, but with external area reduced about 8%. Thus, in a simplistic way, it is estimated that D-shaped tanks would have 8% reduction in heat loss. In fact, considering the influence of thermal stratification, such decrease may be more substantial, as discussed later.

2.2. Physical aspects of the tanks under study

For the numerical simulation two tanks were used, with the same internal volume and the same insulation thickness. The cylindrical tank has internal radius and length of r=0.25 m and z=1.5 m, respectively. As thermal insulation, 0.02 m of expanded polystyrene is used. The D-shaped tank has internal radius and length of R=0.5 m and Z = 0.75 m, respectively. With these dimensions, the external area of the D-shaped tank is approximately 1% less than the cylindrical one.

Moreover, it is assumed that both tanks are found at a room temperature of 20°C and the heat transfer coefficient is $8 W/m^2°C$. The water temperature in the tanks at the beginning of the process is 60°C. In the simulation of hot water consumption, the replacement water temperature was considered at 20°C.

Figure 3 and Figure4 give a view of the computational domain of both tanks, indicating the position of the jet inlet and outlet.

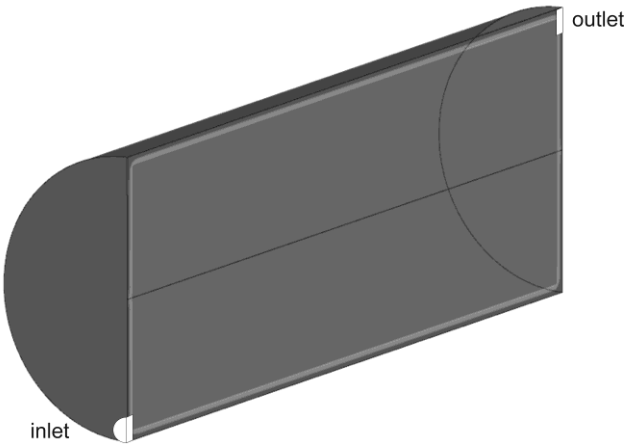

Figure 3. Domain calculation for cylindrical tank

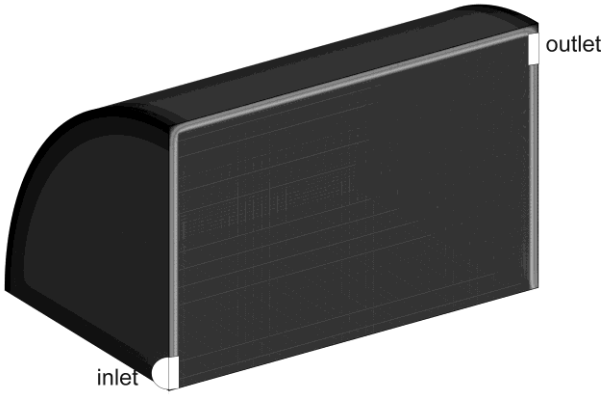

Figure 4. Domain calculation for D-shaped tank

For simulations of the cooling process, the calculation domain was just 1/4 of the physical body, assuming two symmetry planes. Furthermore, for simulations with charge and discharge, the calculation domain was just 1/2 of the physical body, considering the symmetry in the plane through the vertical diameter. The inlet and outlet duct diameters are 0.0254m.

For the determination of the temperature and velocity fields inside the cylindrical horizontal tank, it was necessary to solve the energy and momentum equations in three directions: radial, angular, and axial. In cylindrical coordinates (*r*, θ, *z*) and using the Boussinesq approach, for a Newtonian fluid, the problem was described by the following system of equations:

Continuity equation

$$\frac{1}{r}\frac{\partial}{\partial r}\left(\rho_\infty r V_r\right)+\frac{1}{r}\frac{\partial}{\partial \theta}\left(\rho_\infty V_\theta\right)+\frac{\partial}{\partial z}\left(\rho_\infty V_z\right)=0 \tag{5}$$

where ρ_∞ is the water density calculated at T_{int}.

Momentum equation for the radial velocity component

$$\frac{\partial\left(\rho_\infty V_r\right)}{\partial t}+\frac{1}{r}\frac{\partial\left(\rho_\infty V_\theta V_r\right)}{\partial \theta}+\frac{\partial\left(\rho_\infty V_r V_r\right)}{\partial r}+\frac{\partial\left(\rho_\infty V_z V_r\right)}{\partial z}=$$
$$-\frac{\partial p}{\partial r}+\frac{1}{r^2}\frac{\partial}{\partial \theta}\left(\mu\frac{\partial V_r}{\partial \theta}\right)+\frac{1}{r}\frac{\partial}{\partial r}\left(\frac{\partial\left(\mu r V_r\right)}{\partial r}\right)+\frac{\partial}{\partial z}\left(\mu\frac{\partial V_r}{\partial z}\right)+S^{V_r} \tag{6}$$

where $S^{V_r}=\frac{\rho_\infty V_\theta^2}{r}-\frac{2}{r^2}\frac{\partial}{\partial \theta}\left(\mu V_\theta\right)-\frac{\mu V_r}{r^2}-\left(\rho-\rho_\infty\right)g\cos\left(\theta\right)$ is the source term, μ is the viscosity and β is the thermal expansion coefficient.

Momentum equation for the angular velocity component

$$\frac{\partial\left(\rho_\infty V_\theta\right)}{\partial t}+\frac{1}{r}\frac{\partial\left(\rho_\infty V_\theta V_\theta\right)}{\partial \theta}+\frac{\partial\left(\rho_\infty V_r V_\theta\right)}{\partial r}+\frac{\partial\left(\rho_\infty V_z V_\theta\right)}{\partial z}=$$
$$-\frac{1}{r}\frac{\partial p}{\partial \theta}+\frac{1}{r^2}\frac{\partial}{\partial \theta}\left(\mu\frac{\partial V_\theta}{\partial \theta}\right)+\frac{1}{r}\frac{\partial}{\partial r}\left(\frac{\partial\left(\mu r V_\theta\right)}{\partial r}\right)+\frac{\partial}{\partial z}\left(\mu\frac{\partial V_\theta}{\partial z}\right)+S^{V_\theta} \tag{7}$$

where the source term is $S^{V_\theta}=-\frac{\rho_\infty V_r V_\theta}{r}+\frac{2}{r^2}\frac{\partial\left(\mu V_r\right)}{\partial \theta}-\frac{\mu V_\theta}{r^2}+\left(\rho-\rho_\infty\right)g\,sin\left(\theta\right)\cdot$

Momentum equation for the axial velocity component

$$\frac{\partial\left(\rho_\infty V_z\right)}{\partial t}+\frac{1}{r}\frac{\partial\left(\rho_\infty V_\theta V_z\right)}{\partial \theta}+\frac{\partial\left(\rho_\infty V_r V_z\right)}{\partial r}+\frac{\partial\left(\rho_\infty V_z V_z\right)}{\partial z}=-\frac{\partial p}{\partial z}+\frac{1}{r}\frac{\partial}{\partial r}\left(\mu r\frac{\partial V_z}{\partial r}\right)+\frac{1}{r^2}\frac{\partial}{\partial \theta}\left(\mu\frac{\partial V_z}{\partial \theta}\right)+\frac{\partial}{\partial z}\left(\mu\frac{\partial V_z}{\partial z}\right) \tag{8}$$

With regard to the problem involving charge and discharge, the initial condition for the momentum was zero velocity in the entire domain. The boundary conditions were zero velocity in the external faces and symmetry conditions on the plane rz, described as $V_\theta=0$; $\frac{\partial V_r}{\partial r}=0$ and $\frac{\partial V_z}{\partial r}=0$. Along the line r = 0, the boundary conditions

were $V_\theta = 0$; $V_r = 0$ and $\frac{\partial V_z}{\partial r} = 0$. The solid domain was kept at zero velocity by the imposition of "infinite" viscosity for this volume. For the case without charge and discharge, there was an additional symmetry plane $r\theta$ in the calculation domain, where symmetry conditions described as $V_z = 0$; $\frac{\partial V_r}{\partial z} = 0$ and $\frac{\partial V_\theta}{\partial z} = 0$ were also applied.

Energy Equation

$$\frac{\partial\left(\rho_\infty c_p T\right)}{\partial t} + \frac{1}{r}\frac{\partial\left(\rho_\infty V_\theta c_p T\right)}{\partial \theta} + \frac{\partial\left(\rho_\infty V_r c_p T\right)}{\partial r} + \frac{\partial\left(\rho_\infty V_z c_p T\right)}{\partial z} = \left[\frac{1}{r^2}\frac{\partial}{\partial\theta}\left(k\frac{\partial T}{\partial\theta}\right) + \frac{1}{r}\frac{\partial}{\partial r}\left(kr\frac{\partial T}{\partial r}\right) + \frac{\partial}{\partial z}\left(k\frac{\partial T}{\partial z}\right)\right] + S^T \quad (9)$$

where the term S^T is the source term, also used to incorporate boundary conditions. k and c_p are the thermal conductivity and specific heat at constant pressure of the water, respectively. More details can be found in Savicki *et al.* (2011).

The source term incorporates the overall thermal resistance, including insulation layer and external natural convection, and works as a heat sink in the border volumes.

For the energy equation, the initial condition was the temperature profile prescribed on the fluid region (inside the tank), and a linear variation between the values T_{ini} (on the internal face) and T_{ext} (on the external face) in thermally insulated region. As boundary condition, symmetry was applied on the plane rz and along the line r = 0, $\frac{\partial T}{\partial \theta} = 0$ and $\frac{\partial T}{\partial r} = 0$, respectively. On the outer faces of the tank h_{ext} and T_{ext} were prescribed.

For the inlet and outlet jets, velocity and temperature were imposed. The boundary conditions for the momentum and energy equations, at the inlet jet, were $V_\theta = 0$; $V_r = 0$; $V_z = V_{in}$ and $T = 20°C$. At the outlet jet, boundary conditions were $V_\theta = 0$; $V_r = 0$; $V_z = V_{out}$ and $\frac{\partial T}{\partial z} = 0$. The inlet and outlet velocity are calculated so that the continuity equation is satisfied. Therefore, $V_{in} = Q / A_{in}$ and $V_{out} = Q / A_{out}$, where Q is the volumetric flow rate $\left(m^3 / s\right)$. Due to mesh configuration, the A_{in} e A_{out} are only approximately $\pi D^2 / 4$.

The momentum and energy equations are solved using the Finite Volume Method in cylindrical structured mesh. To solve the algebraic linear equations resulting from the discretization of the governing equations, the TDMA algorithm, with block correction, was employed. In previous studies, the numerical solutions are validated by comparison with experimental data. For interpolation the Power Law scheme was used.

The physical properties of the water (ρ_∞, μ, k, c_p) are uniform in space and updated in time, based on the polynomial fitting as a function of water mean temperature. The variation in the density in space was considered relevant only in the buoyancy term of the momentum equations, and calculated using one polynomial adjusted as a function of temperature at each mesh point. The radiation heat transfer was incorporated in the external convection heat transfer coefficient.

The solution of the transient problem was carried out in a completely implicit form. For each time step, the iterative process was applied until reaching the convergence criterion.

3. NUMERICAL RESULTS

3.1. Simulation of hot water consumption

This study included the two tanks mentioned previously subject to water inlet and outlet in order to measure the hot water consumption by the top and replacing this volume with cold water through the base. The cold water jet enters the bottom of the tank while hot water is extracted (consumption) by the top at a rate of 8 liters per minute. At the initial instant, the water inside the tank is considered to be evenly distributed at 60°C.

The tests of mesh independence and time step were carried out as shown in Tables 1 and 2. The physical time was simulated as 10 minutes.

Table 1. Meshes for cylindrical tank

Cylinder	Mesh 1	Mesh 2	Mesh 3	Mesh 4	Mesh 5
Points in (r,θ,z)	(25,79,75)	(35,105,100)	(40,126,119)	(45,140,134)	(49,153,145)
Time step	0.5	0.1	0.05	0.05	0.05
Total points	148125	367500	599760	844200	1087065

Table 2. Meshes for D-shaped tank

D-shaped tank	Mesh 1	Mesh 2	Mesh 3	Mesh 4	Mesh 5
Points in (r,θ,z)	(50,79,38)	(67,105,50)	(81,126,62)	(91,142,69)	(98,153,75)
Time step	0.5	0.1	0.05	0.05	0.05
Total points	150100	351750	632772	891618	1124550

For mesh 3, Figures 5 and 6 show slices of the distribution of temperature and velocity fields for both tanks.

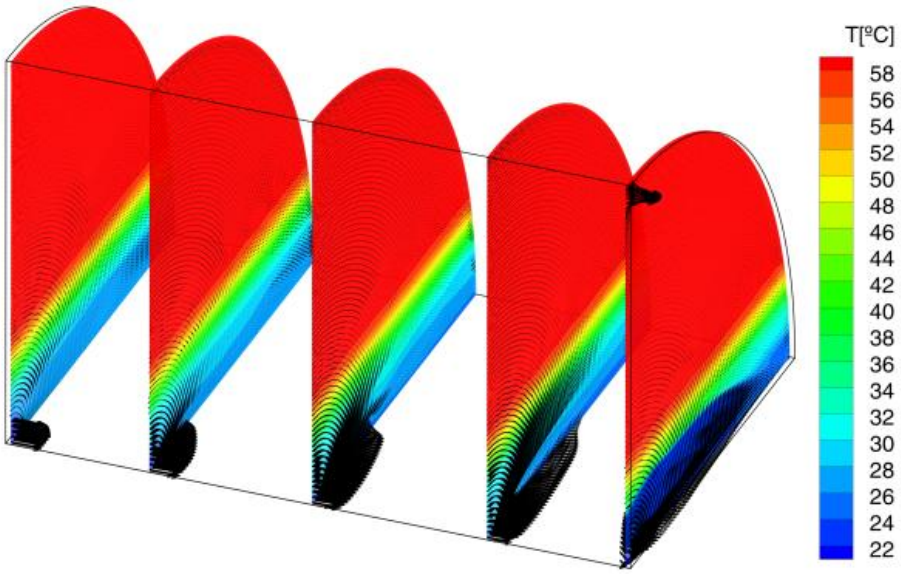

Figure 8. Slices in temperature field for D-shaped tank

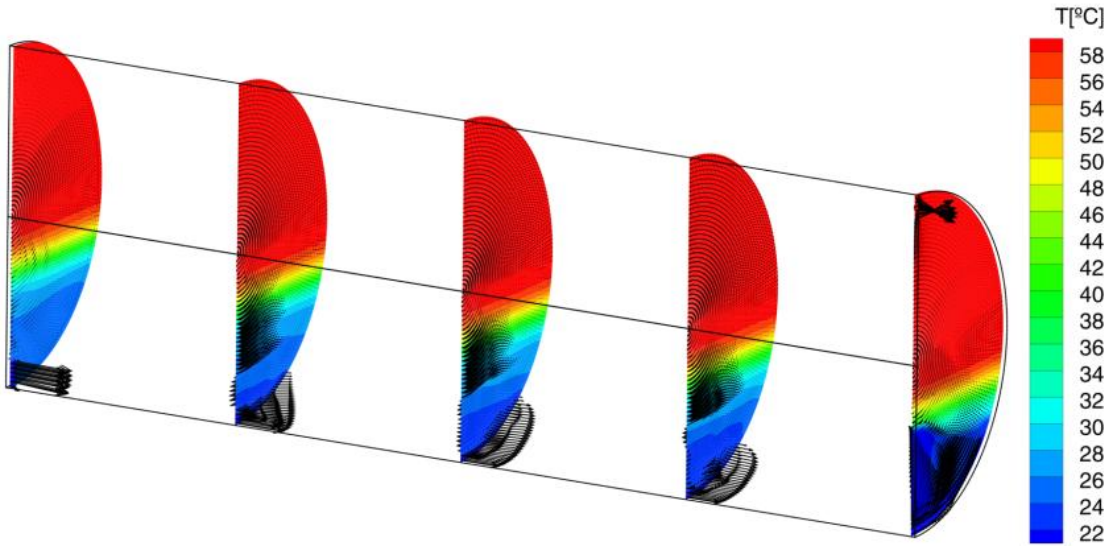

Figure 6. Slices in temperature field for cylindrical tank

There was a strong thermal stratification in both reservoirs. However, there are important differences to be noticed. First, the D-shaped tank showed a more scattered inlet jet, because its bottom is wide and flat. This feature may be particularly important in applications where it is desired to reduce the speed of the inlet jet and thereby reduce turbulence. Second, the D-shaped tank has a larger wetted area bathed with cold water. It means that at the bottom of the D-shaped tank the heat transfer is lesser than that of the corresponding area in the cylindrical tank. In other words, there is a reduced heat loss. If the cooling time is long, this effect can be significant.

Figure 7 gives the temperature profiles for the cylindrical tank obtained after the outlet (consumption) of 80 liters of hot water for the 5 meshes listed in Table 1.

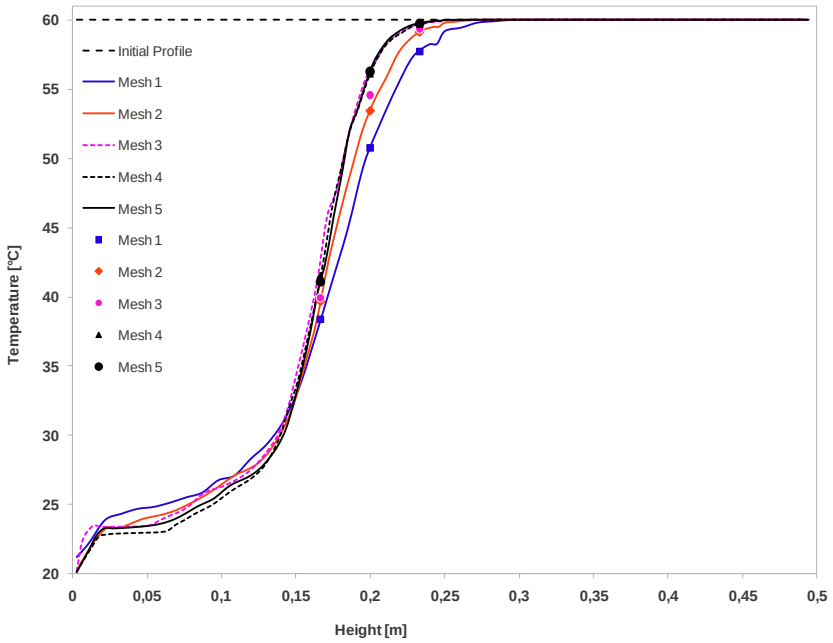

Figure 7. Temperature profiles for the cylindrical tank after 80 liters of hot water consumption

For the D-shaped tank, Figure 8 gives the corresponding temperature profiles obtained after the outlet (consumption) of 80 liters of hot water for the 5 meshes listed in Table 2.

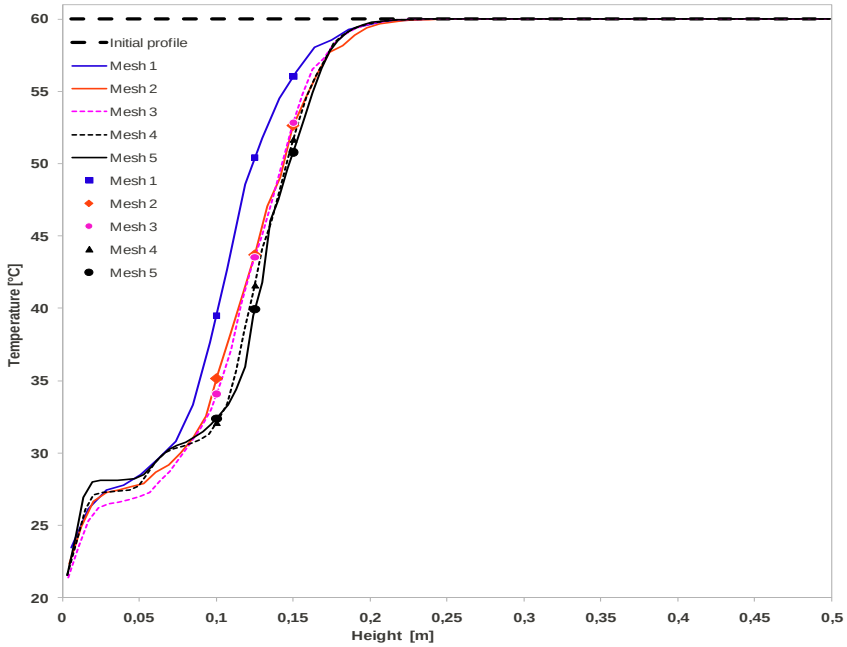

Figure 8. Temperature profiles for the D-shaped after 80 liters of hot water consumption

In Figures 7 and 8, some markers were included in the curves on the points of greatest disagreement. For both tanks, the maximum relative error between the meshes 3 and 4 was less than 0.07, which was considered satisfactory for this study. Therefore, mesh 3 was adopted for the analysis of numerical solutions.

Figure 9 shows the mean temperature in tank obtained at the end of consumption of 80 liters of hot water and inlet of 80 liters of cold water for the 5 meshes tested.

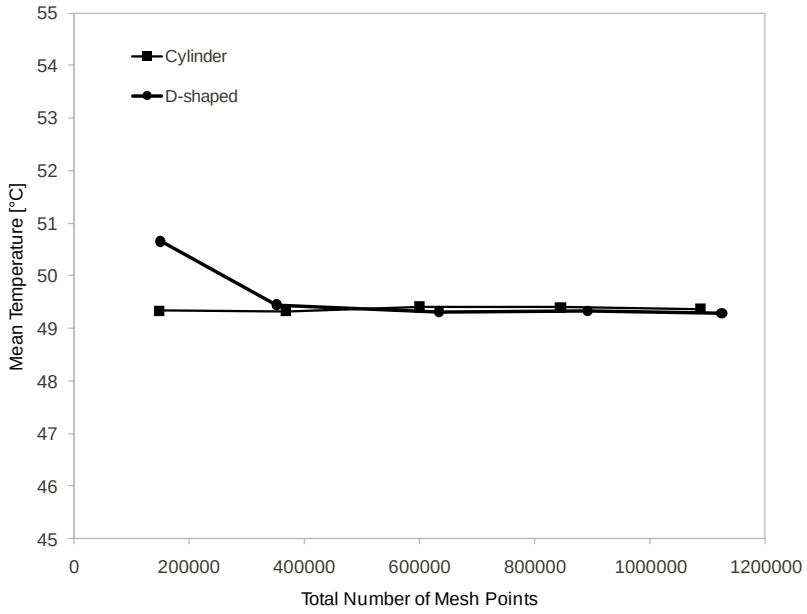

Figure 9. Mesh independency test applied to mean temperature

In the results for mesh 1 there was a significant difference. However, from mesh 2 on the value obtained for the mean temperature agreed satisfactorily.

3.2. Simulation of natural convection

In order to study the behavior of the two tanks subject only to heat loss by natural convection, mesh 3 for both tanks respectively was conducted to numerical simulation for a 10 hour cooling. A case with 2cm of thermal insulation thickness was simulated. Figures 10 and 11 show the temperature field inside the tanks at 10h cooling

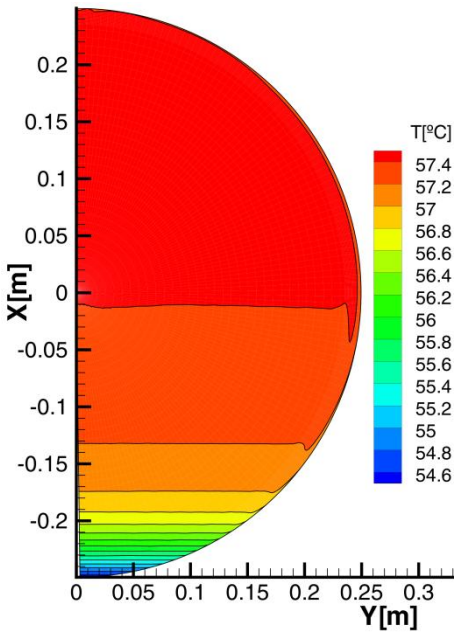

Figure 10. Temperature field in a cross section in the middle of cylindrical tank

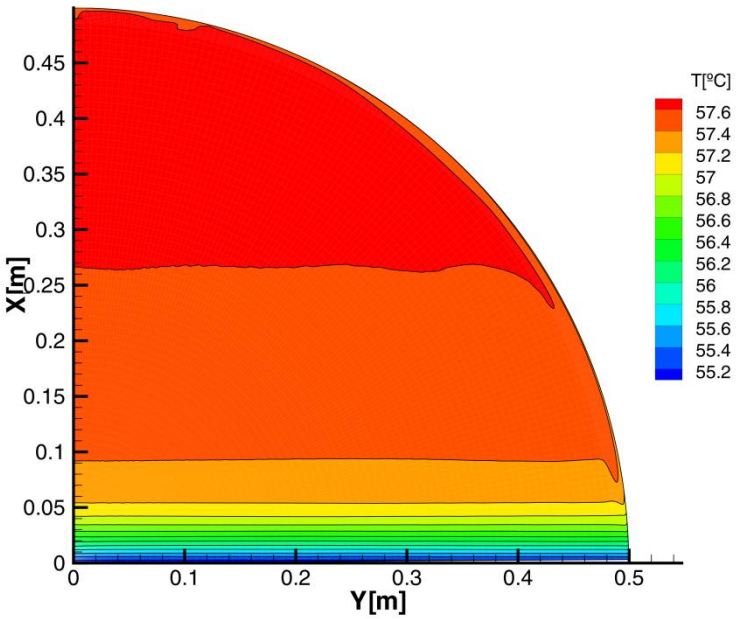

Figure 11. Temperature field in a cross section in the middle of D-shaped tank

As shown in Figures 10 and 11, there were similar vertical profiles of thermal stratification. However, in D-shaped tank, the coldest water at the bottom of the tank is deposited on the widest layer because of the geometry of the tank.

Figures 12 and 13 show the evolution of temperature profiles in time steps of 1 h, for cylindrical and D-shaped tanks respectively.

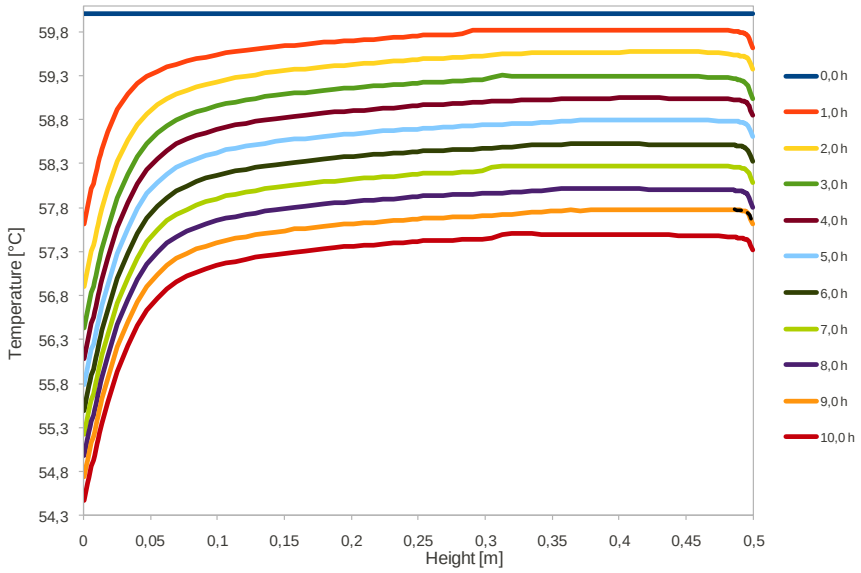

Figure 12. Temperature profiles for cylindrical tank.

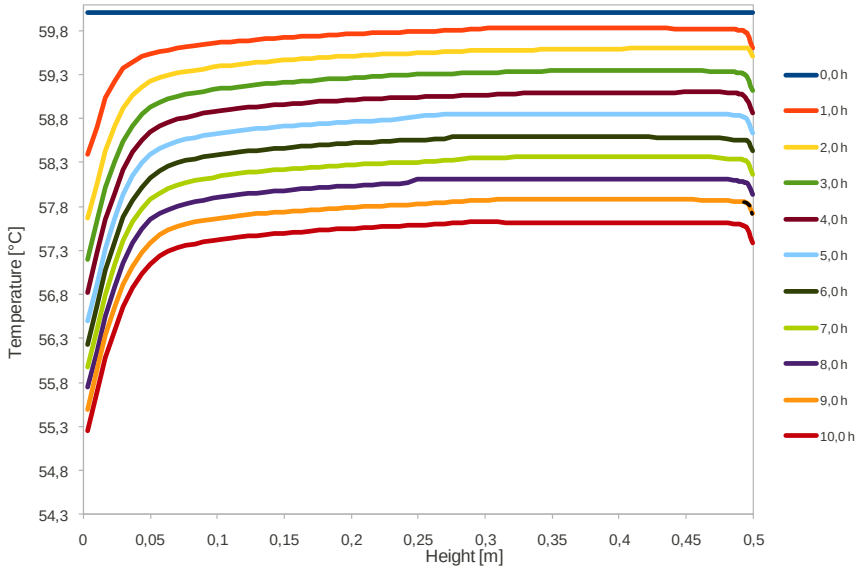

Figure 13. Temperature profiles for D-shaped tank.

The evolution of stratification process was similar in both tanks. After an initial time step, the temperature field becomes stratified and subsequently there is basically a vertical displacement of the temperature profile.

Figure 14 shows a comparison of temperature profiles after 10 h of cooling.

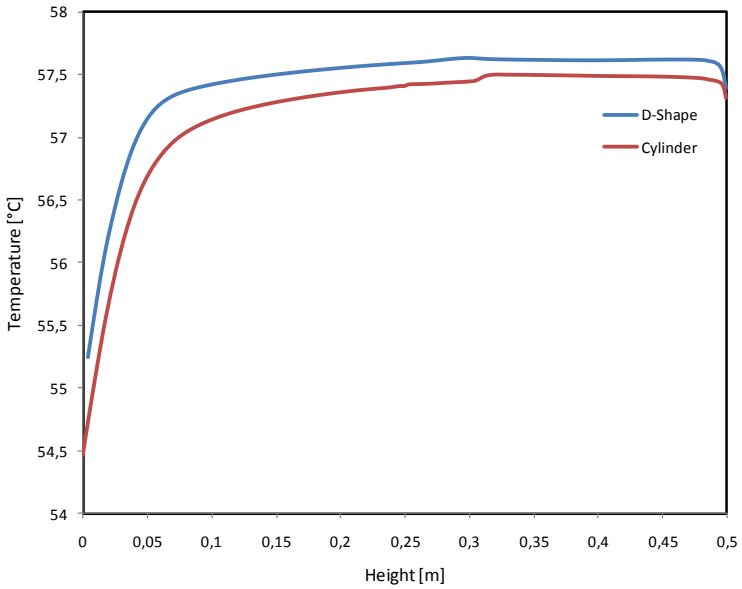

Figure 14. Comparison of temperature profiles at 10 hours for cylindrical and D-shaped tanks.

Although there were similar profiles of thermal stratification, in D-shaped tanks temperatures are slightly higher than in cylindrical ones.

Figure 15 shows the pattern of mean temperature throughout 10 h of simulation. As observed previously, this figure shows that in D-shaped tanks heat loss was slightly lower than in cylindrical ones.

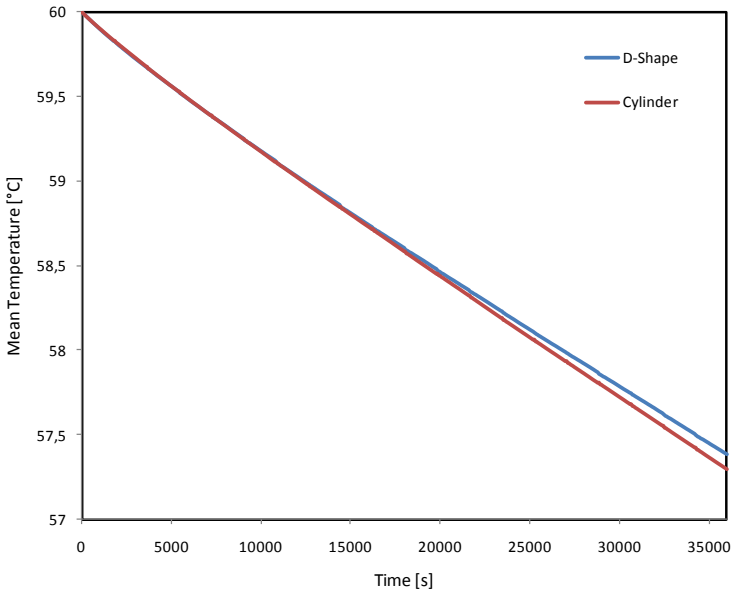

Figure 15. Comparison between mean temperature for cylindrical and D-shaped tanks.

The fact that the mean temperature is slightly higher in D-shaped than in cylindrical tanks may be explained because of the geometry of tanks. That is, the flat bottom of the D-shaped tank provides a larger area bathed by cold water, which reduces the rate of heat transfer. In others words, the mean surface temperature was lower in D-shaped tanks. Furthermore, the cylindrical tank considered with ratio3 has a surface area superior to the D-shaped one, with aspect ratio of 1.5. Thus, the latter has higher heat transfer. As demonstrated in this study, such pattern is expected in cases when the cylindrical tank has high aspect ratio (>2.75), so that it is possible to store in a D-shaped tank the same volume with equal or less surface area.

4. CONCLUSIONS

This study carried out a numerical study of thermal and hydrodynamics behavior of cylindrical and D-shaped tanks was carried out. Two cases were considered, one of hot water consumption and another of natural convection cooling.

The results for simulation of hot water consumption showed that D-shaped tanks reduce the inlet jet speed and thereby reduce turbulence and mixture. Also, D-shaped tanks have a larger wetted area bathed with cold water at the bottom, so that the heat transfer is lower than in cylindrical tanks. That is, there is a reduced heat loss.

For the problem of natural convection cooling, the results showed that the profile of thermal stratification in D-shapes tanks is similar to the cylindrical ones, and that D-shaped tanks cool a bit more slowly than cylindrical ones. However, the conclusions herein presented are dependent on the aspect ratio of the tanks. Therefore, further studies are made necessary with other aspect ratios of tanks. In addition, it is important to study the cooling process for both tanks after hot water consumption and replacement of this volume with cold water.

5. ACKNOWLEDGEMENTS

The authors acknowledge with gratitude the support of the National Council for Scientific and Technological Development – CNPq for their support.

6. REFERENCES

Alizadeh, S., 1999. “An Experimental and Numerical Study of Thermal Stratification in a Horizontal Cylindrical Solar Storage Tank”, Solar Energy, 66, 409-421.

Astrosol, “Boiler Solar”, 23 Feb. 2011, <http://www.astrosol.com.br/boiler_solar.asp>

Fibratec, Reservatório Térmico Solar – Boiler , 23 Feb. 2011, <http://www.fibratec.com.br/index.php>

Consul, R. Rodrigues, I., Perez-Segarra, C. D., Soria, M., 2004. “Virtual Prototyping of Storage Tanks by Means of Three-Dimensional CFD and Heat Transfer Numerical Simulation”, Solar Energy, 77, 179-191.

Duffie, J. A. and Beckman, W. A., 1991, “Solar Engineering of Thermal Processes”, John Wiley & Sons, p.153.

Eames, P. C., Norton, B., 1998. “The Effect of Tank Geometry on Thermally Stratified Sensible Heat Storage Subject to Low Reynolds Number Flow”, Int. J. Heat Mass Transfer. 41, 2131-2142.

Hayase, T. Humphrey, C. Greif, R., 1992. “A Consistently Formulated Quick Scheme for Fast and Stable Convergence Using Finite-Volume Iterative Calculation Procedures”, Journal of Computational Physics, 98, 108-118.

Savicki, D. L. ; Vielmo, H. A. ; Krenzinger, A. “Three-dimensional analysis and investigation of the thermal and hydrodynamic behaviors of cylindrical storage tanks”. Renewable Energy, v. 36, p. 1364-1373, 2011.

Schneider S., Straub, J., 1992. “Laminar Natural Convection in a Cylindrical Enclosure with Different End Temperatures”, International Journal of Heat and Mass Transfer, 35, 545-557.

Shah, L. J., Furbo, S., 2003. “Entrance Effects in Solar Storage Tanks”, Solar Energy, 75, 337-348.

Zachar A., Farkas, I. Szlivka, F., 2003. “Numerical Analyses of the Impact of Plates for Thermal Stratification inside a Storage Tank with Upper and Lower Inlet Flows”, Solar Energy, 74, 287-302.

7. RESPONSIBILITY NOTICE

The authors are the only responsible for the printed material included in this paper.